Research Square

Preprints are preliminary reports that have not undergone peer review.
They should not be considered conclusive, used to inform clinical practice,
or referenced by the media as validated information.

2D-3D Registration for Gait Analysis of Distal Tibiofibular and Tibiotalar Joint Motion

lichao zhang
Beijing Chaoyang Hospital, Capital Medical University
peng su
Shijingshan Teaching Hospital, Capital Medical University
junlin zhou
junlinzhou_article@outlook.com

Beijing Chaoyang Hospital, Capital Medical University

Research Article

Keywords: 2D-3D image registration, Tibiotalar joint, Distal tibiofibular joint, Six degrees of freedom, Kinematics, Gait analysis

Posted Date: July 27th, 2026

DOI: https://doi.org/10.21203/rs.3.rs-9863694/v1

License: This work is licensed under a Creative Commons Attribution 4.0 International License.
Read Full License

Additional Declarations: No competing interests reported.

Abstract

Introdution:

The ankle joint comprises the tibiotalar joint and the distal tibiofibular joint. Although the distal tibiofibular joint has limited motion, its dysfunction significantly affects lower extremity biomechanics. However, the three-dimensional kinematic relationship between these two joints during gait remains unclear.

Methods

The three-dimensional motions of 32 distal tibiofibular joints and tibiotalar joints from 16 healthy adults (8 males, 8 females) were analyzed during normal gait. CT scans were used to create 3D bone models of the tibia, fibula, and talus. X-ray images from seven gait phases were selected for 2D-3D and 3D-3D registration to quantify the six-degree-of-freedom kinematics.

Results

During gait, distinct kinematic patterns were observed in both joints. In the distal tibiofibular joint, the fibula exhibited rotational ranges of motion (ROM) of 0.67 ± 0.27° (plantarflexion/dorsiflexion), 0.18 ± 0.1° (inversion/eversion), and 1.18 ± 0.62° (internal/external rotation). Translational ROMs were 1.95 ± 0.79 mm (medial/lateral), 2.65 ± 1.13 mm (anterior/posterior), and 1.91 ± 1.12 mm (superior/inferior). In the tibiotalar joint, internal–external rotation (ROM: 15.53° ± 6.08°) and plantarflexion–dorsiflexion (ROM: 14.92° ± 5.71°) were the predominant motions. Talar motion exhibited strong coupling: plantarflexion was highly correlated with anterior and inferior translation (r = 0.85), whereas dorsiflexion was highly correlated with posterior and superior translation.

Conclusion

The distal tibiofibular joint exhibits coupled motion with the tibiotalar joint during normal gait, though independent movement patterns persist. These six-DOF kinematic data provide an in vivo reference for understanding ankle joint biomechanics.

Introdution

In vivo assessment of ankle joint movement is essential for understanding normal and pathological foot mechanics, evaluating injury effects, and assessing surgical outcomes [1]. The ankle joint comprises the tibiotalar joint and the talofibular joint, with stability maintained by the talofibular complex at the distal tibiofibular junction. This fibrous complex consists of four structures: the anterior inferior tibiofibular ligament, posterior inferior tibiofibular ligament, transverse ligament, and interosseous membrane [2].

Among these, the posterior inferior tibiofibular ligament plays a key role in resisting external rotation forces [3].

Precise measurement of the tibiotalar and talofibular joints—whether normal, pathological, or postoperative—can help elucidate the mechanisms of ankle osteoarthritis. However, accurate in vivo measurement remains challenging. Skin marker-based motion analysis requires assuming tibiofibular rigidity due to the lack of suitable cutaneous landmarks around the talus. Intracortical pins with reflective markers can independently track tibial and talar motion but are highly invasive [4]. Dynamic MRI offers precise measurements but is limited to small sample sizes and confined spaces that preclude physiological loading [5].

In vitro studies using fresh-frozen cadavers have explored tibiofibular motion under non-weight-bearing conditions [6][7]; however, they cannot replicate real gait or reflect normal in vivo physiology. Surface markers suffer from skin-bone artifact, while bone pins cause invasive trauma and raise ethical concerns [8].

Two-dimensional-to-three-dimensional (2D-3D) image registration has proven effective for bone and joint kinematic measurement. Recent studies have increasingly applied this technique. Paulus et al. used dual-plane registration to measure ankle and subtalar joint axes during walking and running [9]. Yang et al. applied 3D/2D dual-plane registration to analyze sex- and side-related differences in ankle and hindfoot motion [10]. Yamazaki et al. used 2D-3D registration to assess total knee arthroplasty kinematics [11]. Chen Wang et al. applied feature-based 2D-3D registration to analyze distal tibiofibular joint motion during walking [12].

Despite its utility, 2D-3D registration has inherent errors. Zhu et al. employed dual-plane registration to improve accuracy over single-plane methods [13]. De Bruin et al. proposed a radiographic stereometric analysis validated with opaque markers, which is now used as a verification method for 2D-3D registration [14].

The purpose of this study is to use 2D-3D registration to investigate the in vivo three-dimensional motion patterns of the tibiotalar and distal tibiofibular joints during the normal gait cycle. Ankle and hindfoot kinematics are of great significance for total ankle replacement design and for estimating muscle forces in musculoskeletal models.

Methods

Study population

Sixteen healthy adults (8 males, 8 females) were enrolled. The mean age was 38.75 ± 16.18 years, mean height 1.68 ± 0.10 m, mean weight 68.81 ± 12.10 kg, and mean BMI 24.35 ± 4.41.

Inclusion criteria were: healthy adults; normal physical development and gait; normal lower limb alignment and arch development; no ligamentous hyperlaxity; no history of chronic lower limb pain, limited mobility, fractures, or surgeries; ability to cooperate; and signed informed consent.

Exclusion criteria were: abnormal lower limb development or alignment; ligamentous hyperlaxity; arch abnormalities (high arch or flat foot); history of chronic pain, limited mobility, fractures, or surgeries; or inability to cooperate.

Ethical approval

and radiation safety

All volunteers provided written informed consent. The study was approved by the Ethics Committee of Beijing Shijingshan Hospital (Approval No.: sjsky-202101).

CT imaging and 3D model reconstruction

CT scans (Discovery CT750HD, GE, USA) covered the full lengths of the tibia, fibula, and talus. Parameters: slice thickness 0.625 mm; voltage 120 kV; current 200 mA; matrix 512 × 512 pixels. Bone contours were segmented based on bone-soft tissue density differences. Three-dimensional models of the tibia, fibula, and talus were reconstructed using Mimics software (Mimics Innovation Suite 21, Materialise NV, Leuven, Belgium) (Fig. 1). An anatomical coordinate system [15] and the coordinate system defined by Yamaguchi et al. [16] were established. Axis directions followed the right-hand rule.

Gait image acquisition

A digital multifunctional X-ray fluoroscopy system (SHIMADZU, SONIALVISION G4, Japan) captured the tibia, fibula, and talus during walking. The gait cycle was defined from heel strike to the subsequent ipsilateral heel strike, comprising support and swing phases. Gait was divided into seven typical phases (Fig. 2).

Image registration

A three-dimensional virtual environment containing the 3D bone models, X-ray images, and virtual radiation sources was created in Mimics. The segmented tibia, fibula, and talus could independently translate and rotate with six degrees of freedom (DOF). Using the X-ray module, each 3D bone model was projected onto 2D lateral X-ray images, and 2D-3D multimodal registration was performed based on image feature contours (Fig. 3). Subsequently, 3D-3D registration of the tibia, fibula, and talus in different postures was conducted in 3-matic software (Fig. 4).

The registration procedure consisted of five steps: (1) manual registration of X-rays; (2) manual registration of the tibia, fibula, and talus; (3) selection of the contours of the tibia, fibula, and talus; (4) automatic 2D-3D registration based on contour features; (5) automatic 3D-3D registration, with the fibula and talus registered sequentially relative to the tibia.

Kinematic analysis

The six-DOF spatial positions and orientations of the tibia, fibula, and talus were determined. Aligned 3D models were imported into 3-matic 13.0 (Materialise NV). The resting position of the fibula and talus served as the reference. Relative motions were calculated via decomposition of XYZ anatomical coordinates. Axis definitions: X-axis – medial/lateral translation; Y-axis – anterior/posterior translation; Z-axis – superior/inferior translation. Rotations followed the right-hand rule: α – plantarflexion/dorsiflexion; β – inversion/eversion; γ – external/internal rotation (Fig. 5).

For each DOF, the mean range of motion (ROM) was calculated as the average across all 32 joints (16 participants × 2 sides). The mean joint position for each of the seven postures was similarly averaged across all joints.

Results

Overall range of motion

The mean ranges of motion (ROM) for the fibula and talus during the gait cycle are summarized in Tables 1 and 2. The kinematic patterns for each degree of freedom are shown in Figs. 6.

Table 1
Range of Motion (ROM) of the fibula at each degree of freedom during the seven postures of the gait cycle.

Movements	The fibula ROM(Average ± Standard Deviation)
Dorsiflexion/Palmarflexion	0.67°±0.27°
Internal/External Rotation	1.18°±0.62°
Inversion/Eversion	0.18°±0.1°
Superior/Inferior	1.91 ± 1.12 mm
Medial/Lateral	1.95 ± 0.79 mm
Anterior/Posterior	2.65 ± 1.13 mm

Table 2
Range of Motion (ROM) of the talus at each degree of freedom during the seven postures of the gait cycle

Movements	The talus ROM(Average ± Standard Deviation)
Dorsiflexion/Palmarflexion	14.92°±5.71°
Internal/External Rotation	15.53°±6.08°
Inversion/Eversion	9°±4.35°
Superior/Inferior	2.51 ± 1.25
Medial/Lateral	2.59 ± 1.47
Anterior/Posterior	5.63 ± 1.98

Distal tibiofibular joint. Relative to the tibia, the fibula exhibited rotational ROMs of 0.67 ± 0.27° (plantarflexion/dorsiflexion), 0.18 ± 0.1° (inversion/eversion), and 1.18 ± 0.62° (internal/external rotation). Translational ROMs of the distal fibula were 1.95 ± 0.79 mm (medial/lateral), 2.65 ± 1.13 mm (anterior/posterior), and 1.91 ± 1.12 mm (superior/inferior) (Table 1).

Tibiotalar joint. Relative to the tibia, the talus demonstrated rotational ROMs of 14.92 ± 5.71° (plantarflexion/dorsiflexion), 9 ± 4.35° (inversion/eversion), and 15.53 ± 6.08° (internal/external rotation). Translational ROMs were 2.59 ± 1.47 mm (medial/lateral), 5.63 ± 1.98 mm (anterior/posterior), and 2.51 ± 1.25 mm (superior/inferior) (Table 2).

Three-dimensional motion of the distal tibiofibular joint

From heel contact preparation to mid-stance (postures 1–4), the fibula dorsiflexed by 0.46°, everted by 0.09°, and externally rotated by 0.27° relative to the tibia. Concurrently, the distal fibula translated 1.8 mm laterally, 1.91 mm anteriorly, and 0.29 mm superiorly.

From mid-stance to toe-off (postures 4–7), the fibula underwent 0.01° of plantarflexion, 0.04° of inversion, and 0.13° of internal rotation. The distal fibula translated 1.44 mm medially, 0.88 mm posteriorly, and 0.52 mm inferiorly(Table 3).

Table 3
Average rotation angles and average displacement of the fibula at each degree of freedom during the seven postures of the gait cycle.

Movement	Posture 1	Posture 2	Posture 3	Posture 4	Posture 5	Posture 6	Posture 7
Plantarflexion (-) / Dorsiflexion (+)	-0.05°± 0.27°	0.01°± 0.28°	0.3°± 0.27°	0.41°± 0.27°	0.37°± 0.21°	0.41°± 0.2°	0.4°± 0.21°
Inversion (-) / Eversion (+)	-0.03°± 0.08°	0.01°± 0.08°	0.06°± 0.08°	0.06°± 0.08°	0.05°± 0.07°	0.04°± 0.07°	0.02°± 0.07°
Internal (+) / External Rotation (-)	0.77°± 0.53°	0.76°± 0.5°	0.62°± 0.47°	0.5°± 0.41°	0.56°± 0.41°	0.64°± 0.4°	0.63°± 0.24°
Superior (+) / Inferior (-)	-0.75 ± 0.77 mm	-0.88 ± 0.81 mm	-0.61 ± 0.83 mm	-0.46 ± 0.86 mm	-0.57 ± 0.77 mm	-0.98 ± 0.79 mm	-0.45 ± 0.81 mm
Medial (+) / Lateral (-)	-0.02 ± 0.36 mm	0.32 ± 0.36 mm	1.21 ± 0.35 mm	1.78 ± 0.39 mm	1.05 ± 0.47 mm	0.72 ± 0.45 mm	0.34 ± 0.42 mm
Anterior (+) / Posterior (-)	-0.23 ± 1.10 mm	-0.21 ± 1.12 mm	1.10 ± 1.12 mm	1.69 ± 1.07 mm	1.04 ± 0.71 mm	1.08 ± 0.68 mm	0.81 ± 0.52 mm

Three-dimensional motion of the tibiotalar joint

From heel contact preparation to mid-stance (postures 1–4), the talus relative to the tibia showed the following patterns:

- In the sagittal plane, maximal dorsiflexion (25.27°) occurred at posture 2, decreased at posture 3, and increased again at posture 4. Anterior translation peaked at posture 2 (5.02 mm).
- In the coronal plane, maximal eversion (14.46°) was observed at posture 2.
- In the horizontal plane, maximal external rotation (− 7.82°) occurred at posture 2, approached neutral at posture 3, and slightly increased thereafter(Table 4).

Table 4
average rotational angle and average displacement of the talus at each degree of freedom during the seven postures in the gait cycle.

Movement	Posture 1	Posture 2	Posture 3	Posture 4	Posture 5	Posture 6	Posture 7
Plantarflexion (-) / Dorsiflexion (+)	21.46°± 10.68°	25.27°± 9.07°	18.36°± 8.17°	22.47°± 7.24°	20.16°± 9.69°	20.75°± 10.65°	23.93°± 8.95°
Inversion (-) / Eversion (+)	11.91°± 6.29°	14.46° ±5.82°	10.78° ±2.54°	13.96° ±5.82°	11.13°± 5.6°	10.88°± 6.15°	13.18°± 5.7°
Internal (+) / External Rotation (-)	-5.73°± 8.82°	-7.82° ± 7.98°	-1.75° ± 7.52°	-2.45° ± 7.03°	0.77°± 7.06°	-1.02°± 7.66°	-1.22°± 7.4°
Superior (+)/ Inferior (-)	4.16 ± 1.97 mm	5.02 ± 1.77 mm	4.02 ± 1.69 mm	4.70 ± 1.87mmm	4.13 ± 2.01 mm	4.11 ± 2.23 mm	4.4 ± 2.11 mm
Medial (+) / Lateral (-)	-3.28 ± 1.44 mm	-3.56 ± 1.45 mm	-2.85 ± 1.27 mm	3.3 ± 1.45 mm	-2.96 ± 1.69 mm	3.07 ± 1.65mmm	-3.31 ± 1.56 mm
Anterior (+)/ Posterior (-)	-6.66 ± 3.29 mm	-8.09 ± 2.6 mm	-5.33 ± 2.32 mm	-6.78 ± 2.04 mm	-5.88 ± 2.72 mm	-6.1 ± 3.32 mm	-7.53 ± 2.7 mm

Correlations between joint motions

Within the distal tibiofibular joint. Fibular internal/external rotation was moderately correlated with inversion/eversion (r = 0.55) and dorsiflexion/plantarflexion (r = 0.48)

Within the tibiotalar joint. Talar inversion/eversion was highly correlated with dorsiflexion/plantarflexion (r = 0.82) and superior/inferior translation (r = 0.70). Talar dorsiflexion/plantarflexion was highly correlated with superior/inferior translation (r = 0.85)

Between the distal tibiofibular and tibiotalar joints. Talar internal–external rotation was weakly correlated with fibular anterior–posterior translation (r = 0.20) and fibular dorsiflexion–plantarflexion (r = 0.16) (Table 5).

Table 5
The correlation of movement between the distal tibiofibular joint and the Tibio-talar joint

Fibula movement pattern	Fibula movement pattern	Correlation coefficient	P value
Internal (+) / External Rotation (-)	Eversion (+)/Inversion (-)	0.55	< 0.001
Internal (+) / External Rotation (-)	Dorsiflexion(+)/Plantarflexion (-)	0.48	< 0.001
Internal (+) / External Rotation (-)	Superior (+) / Inferior (-)	-0.39	< 0.001
Eversion (+)/Inversion (-)	Anterior (+) / Posterior (-)	0.40	< 0.001

Talus movement pattern	Talus movement pattern	Correlation coefficient	P value
Internal (+) / External Rotation (-)	Eversion (+)/Inversion (-)	-0.63	< 0.001
Eversion (+)/Inversion (-)	Dorsiflexion(+)/Plantarflexion (-)	0.82	< 0.001
Dorsiflexion(+)/Plantarflexion (-)	Superior (+) / Inferior (-)	0.85	< 0.001
Eversion (+)/Inversion (-)	Superior (+) / Inferior (-)	0.70	< 0.001
Eversion (+)/Inversion (-)	Anterior (+) / Posterior (-)	-0.72	< 0.001

Talus movement pattern	Fibula movement pattern	Correlation coefficient	P value
Internal (+) / External Rotation (-)	Anterior (+) / Posterior (-)	0.20	0.004
Internal (+) / External Rotation (-)	Dorsiflexion(+)/Plantarflexion (-)	0.16	0.024
Internal (+) / External Rotation (-)	Eversion (+)/Inversion (-)	0.13	0.065

Discussion

This study used 2D-3D registration to non-invasively investigate the in vivo kinematics of the distal tibiofibular and tibiotalar joints during the gait cycle. This method has been validated for assessing sacroiliac screw loosening [17] and lumbar spine alignment [18], with segmentation errors < 1 mm [18].

Several cadaveric studies have examined talofibular motion. Bozkurt et al. [19] reported that the fibula moves posterior-to-anterior during plantar-to-dorsiflexion. Weinert [20] observed downward and lateral fibular displacement during weight-bearing. Our previous work [21] and that of Chen Wang et al. [12] demonstrated similar fibular motion patterns during gait.

Our results show fibular rotational ROMs of 0.67 ± 0.27° (plantarflexion/dorsiflexion), 0.18 ± 0.1° (inversion/eversion), and 1.18 ± 0.62° (internal/external rotation), consistent with Alves [22] and Soavi et al. [23], who reported fibular rotation < 2°. For the tibiotalar joint, our ROMs align with Mako et al. [24], who also found greater ROM in females.

Our results revealed strong coupling within the tibiotalar joint: plantarflexion was coupled with internal rotation and inversion, while dorsiflexion was coupled with external rotation and eversion. This coupling was highly correlated with talar translations: plantarflexion with anterior and inferior translation, and dorsiflexion with posterior and superior translation—consistent with the anatomical constraints of the ankle joint.

Within the distal tibiofibular joint, fibular internal rotation was accompanied by eversion, and external rotation by inversion—mirroring the talar rotation–inversion coupling and reflecting the integrity of the ankle mortise.

We observed weak but significant correlations between tibiotalar and distal tibiofibular joint motions. Talar internal rotation correlated with fibular anterior translation ($r = 0.20$) and dorsiflexion ($r = 0.16$). Overall, rotation and displacement are highly coordinated in the ankle, consistent with its characterization as a "compound hinge joint."

Clinical implications

Our findings have several clinical implications. First, the observed dominant internal–external rotation and anterior–posterior translation of the fibula during gait inform the debate regarding elastic versus rigid fixation for distal tibiofibular joint injuries. Second, reduced coordination of ankle joint motions may serve as an indicator of ligament injury. Third, rehabilitation protocols can be designed based on the identified coupled motion patterns. Finally, the coupled motion between the two joints may guide the design of ankle prostheses.

Limitations

This study has several limitations. First, the sample size (16 volunteers, 32 limbs) was relatively small. Second, the registration process requires user experience and manual contour selection, which may introduce bias. Third, single-plane X-rays were used due to equipment constraints; dual-plane orthogonal imaging would improve registration accuracy. However, previous studies [12][21][25] have validated 2D-3D single-plane registration, with rotation errors < 0.5° and translation errors < 0.2 mm[21].

Conclusion

Understanding the physiological motion of the tibiotalar and distal tibiofibular joints during gait is fundamental for studying complex lower limb movements. Our six-DOF kinematic data provide an in vivo reference for future research on ankle joint motion and for clinical diagnosis, treatment, and evaluation of ankle disorders.

Declarations

Author Contribution

L.Z. and P.S. conceived and designed the study. L.Z. performed the experiments and analyzed the data. P.S. and J.Z. prepared figures and tables. L.Z. and J.Z. wrote the main manuscript text. All authors reviewed and approved the final manuscript.

1.Clinical trial registration: Not applicable.

2.Ethics approval: Approved by the Institutional the Ethics Committee of Beijing Shijingshan Hospital (Approval No.: sjsky-202101). Performed in accordance with the Declaration of Helsinki.

3.Consent to participate: Written informed consent was obtained from all participants.

4.Funding: No funding was received

References

1. Hintermann B, Boss A, Schäfer D. Arthroscopic findings in patients with chronic ankle instability. Am J Sports Med. 2002;30(3):402–9.
2. Liu J, Liu Y, Huang Q, et al. Management of syndesmosis injury: a narrative review. Orthop Res Rev. 2022;14:471–5.
3. Khambete P, Hosseini A, Akbari-Shandiz M, et al. Biomechanics of the distal tibiofibular syndesmosis: a systematic review of cadaveric studies. Foot Ankle Orthop. 2021;6(2):24730114211012701.
4. Kobayashi T, Suzuki D, Kamo K, et al. In vivo kinematics of the talocrural and subtalar joints with functional ankle instability during weight-bearing ankle internal rotation: a pilot study. Foot Ankle Spec. 2013;6(3):178–84.
5. Clarke EC, Martin JH, d'Entremont AG, et al. A non-invasive, 3D, dynamic MRI method for measuring muscle moment arms in vivo: demonstration in the human ankle joint and Achilles tendon. Med Eng Phys. 2015;37(1):93–9.
6. Wang Q, Whittle M, Cunningham J, Kenwright J. Fibula and its ligaments in load transmission and ankle joint stability. Clin Orthop Relat Res. 1996;(330):261–70.
7. Hogg-Cornejo V, Hunt KJ, Bartolomei J, et al. Normal kinematics of the syndesmosis and ankle mortise during dynamic movements. Foot Ankle Orthop. 2020;5(3):2473011420933007.

8. Alves-da-Silva T, Guerra-Pinto F, Matias R, Pessoa P. Kinematics of the proximal tibiofibular joint is influenced by ligament integrity, knee and ankle mobility: an exploratory cadaver study. Knee Surg Sports Traumatol Arthrosc. 2019;27(2):405–11.
9. Paulus P, Saliba A, Kiapour A, et al. Ankle and subtalar joint axes of rotation and center of rotation during walking and running in healthy individuals measured using dynamic biplane radiography. J Biomech. 2023;160:111837.
10. Yang S, Wimberly K, Zhang X, et al. Healthy ankle and hindfoot kinematics during gait: sex differences, asymmetry and coupled motion revealed through dynamic biplane radiography. J Biomech. 2021;116:110220.
11. Yamazaki T, Watanabe T, Nakajima Y, et al. 3D kinematics of mobile-bearing total knee arthroplasty using X-ray fluoroscopy. Int J Comput Assist Radiol Surg. 2015;10(4):487–95.
12. Wang C, Yang J, Wang S, et al. Three-dimensional motions of distal syndesmosis during walking. J Orthop Surg Res. 2015;10:166.
13. Zhu Z, Li G. An automatic 2D-3D image matching method for reproducing spatial knee joint positions using single or dual fluoroscopic images. Comput Methods Biomech Biomed Engin. 2012;15(11):1245–56.
14. de Bruin PW, Kaptein BL, Stoel BC, et al. Image-based RSA: roentgen stereophotogrammetric analysis based on 2D-3D image registration. J Biomech. 2008;41(1):155–64.
15. Wu G, Siegler S, Allard P, et al. ISB recommendation on definitions of joint coordinate system of various joints for the reporting of human joint motion—part I: ankle, hip, and spine. J Biomech. 2002;35(4):543–8.
16. Yamaguchi S, Sasho T, Kato H, et al. Ankle and subtalar kinematics during dorsiflexion-plantarflexion activities. Foot Ankle Int. 2009;30(4):361–6.
17. Pieroh P, Lenk M, Hohmann T, et al. Intra- and interrater reliabilities and a method comparison of 2D and 3D techniques in cadavers to determine sacroiliac screw loosening. Sci Rep. 2019;9(1):3141.
18. Hajnal B, Eltes PE, Bereczki F, et al. New method to apply the lumbar lordosis of standing radiographs to supine CT-based virtual 3D lumbar spine models. Sci Rep. 2022;12(1):20382.
19. Bozkurt M, Tonuk E, Elhan A, et al. Axial rotation and mediolateral translation of the fibula during passive plantarflexion. Foot Ankle Int. 2008;29(5):502–7.
20. Weinert CR Jr, McMaster JH, Ferguson RJ. Dynamic function of the human fibula. Am J Anat. 1973;138(2):145–9.
21. Zhang L, Su P, Zhou J. Tibia-fibula relative motion during gait cycle by 2D-3D registration. J Orthop Res. 2025;43(11):1987–96.
22. Alves-da-Silva T, Guerra-Pinto F, Matias R, Pessoa P. Kinematics of the proximal tibiofibular joint is influenced by ligament integrity, knee and ankle mobility. Knee Surg Sports Traumatol Arthrosc. 2019;27(2):405–11.

23. Soavi R, Girolami M, Loreti I, et al. The mobility of the proximal tibio-fibular joint: a roentgen stereophotogrammetric analysis on six cadaver specimens. Foot Ankle Int. 2000;21(4):336–42.
24. Fukano M, Fukubayashi T, Banks SA. Sex differences in three-dimensional talocrural and subtalar joint kinematics during stance phase in healthy young adults. Hum Mov Sci. 2018;61:117–25.
25. Lawrence RL, Ellingson AM, Ludewig PM. Validation of single-plane fluoroscopy and 2D/3D shape-matching for quantifying shoulder complex kinematics. Med Eng Phys. 2018;52:69–75.

Figures

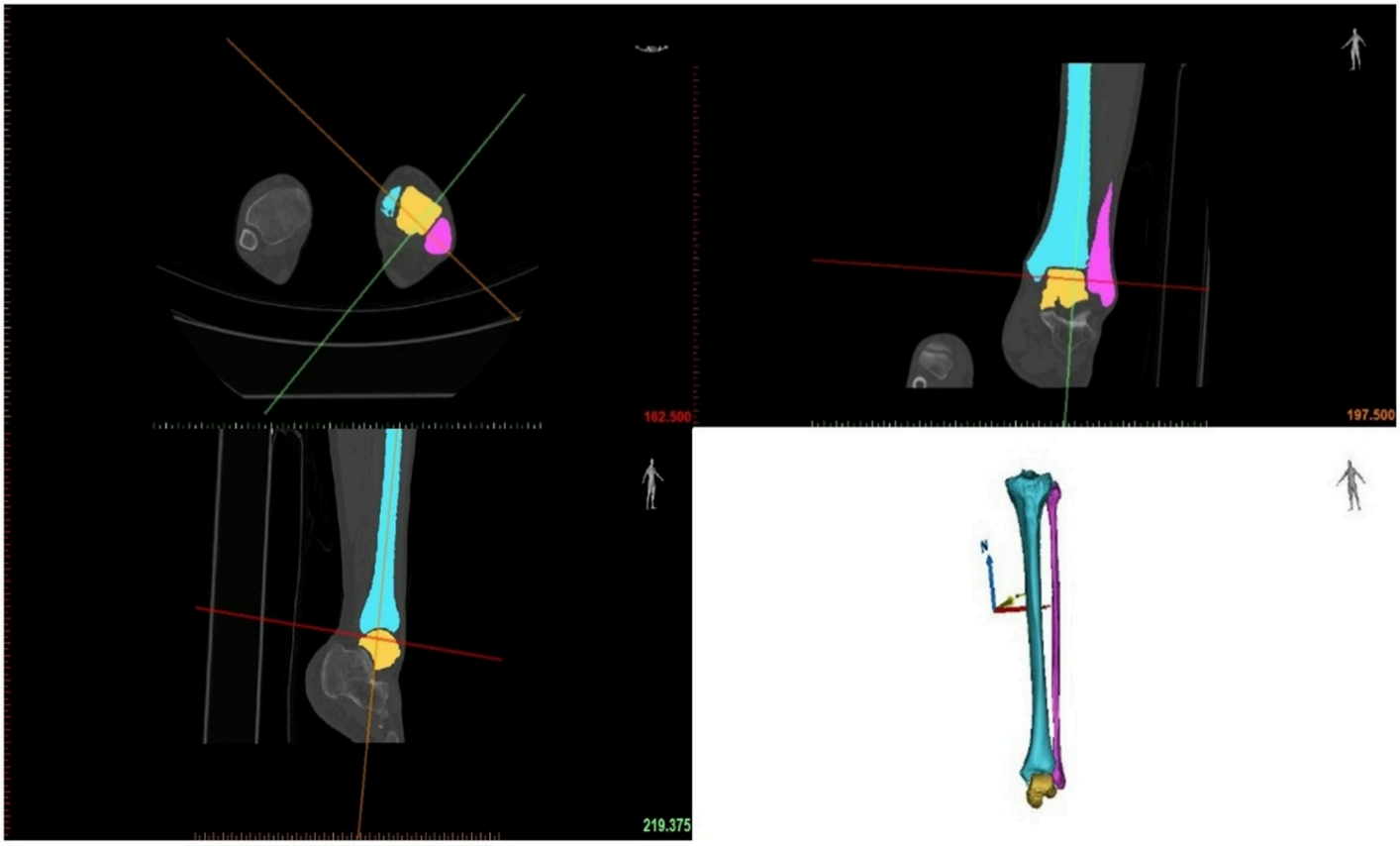


Figure 1

Image segmentation of the tibia, fibula and talus

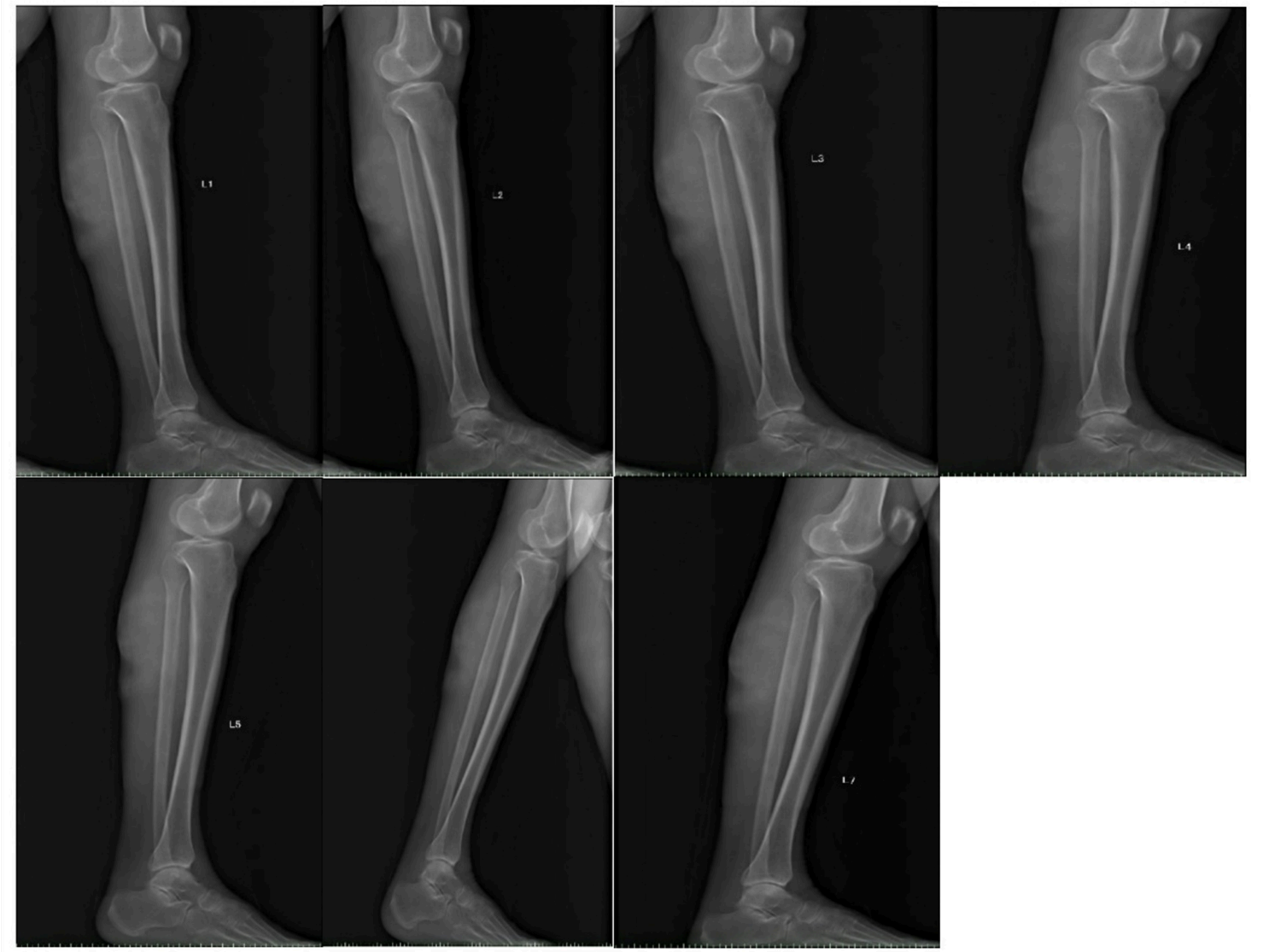


Figure 2

Seven Key Movements in the Gait Cycle



Figure 3

Steps of 2D-3D Registration Based on Image Contours

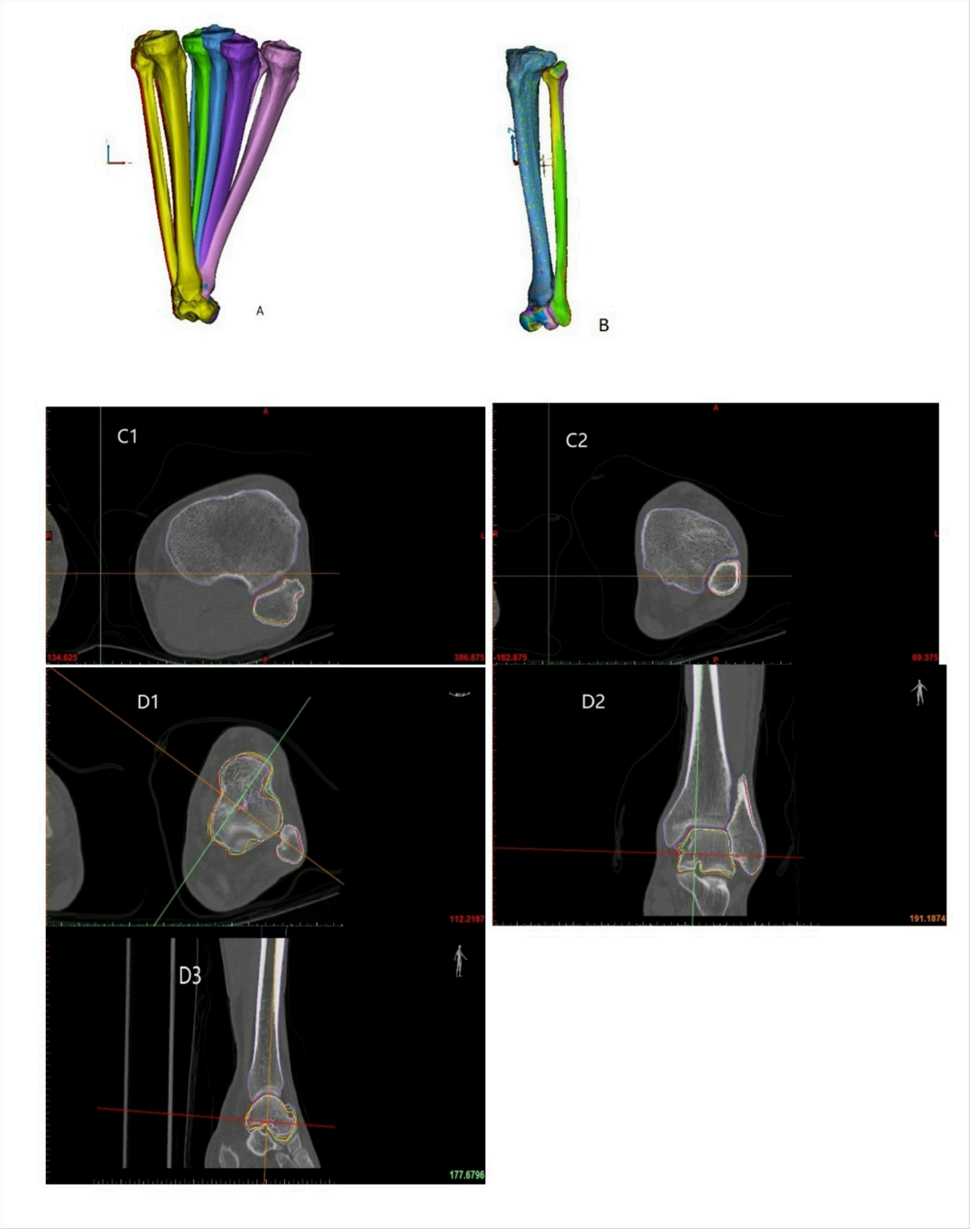


Figure 4

A. The relative positions of the tibia, fibula and talus during the gait cycle. B. 3D-3D registration of the tibia, with the fibula and talus following the tibia during the registration process. C. The tibia has completed 3D registration, and the relative positions of the proximal end of the fibula (C1) and the distal end of the fibula (C2) have changed. D. The tibia has completed 3D registration, and the relative position

of the talus has changed, in the transverse position (D1), coronal position (D2), and sagittal position (D3).

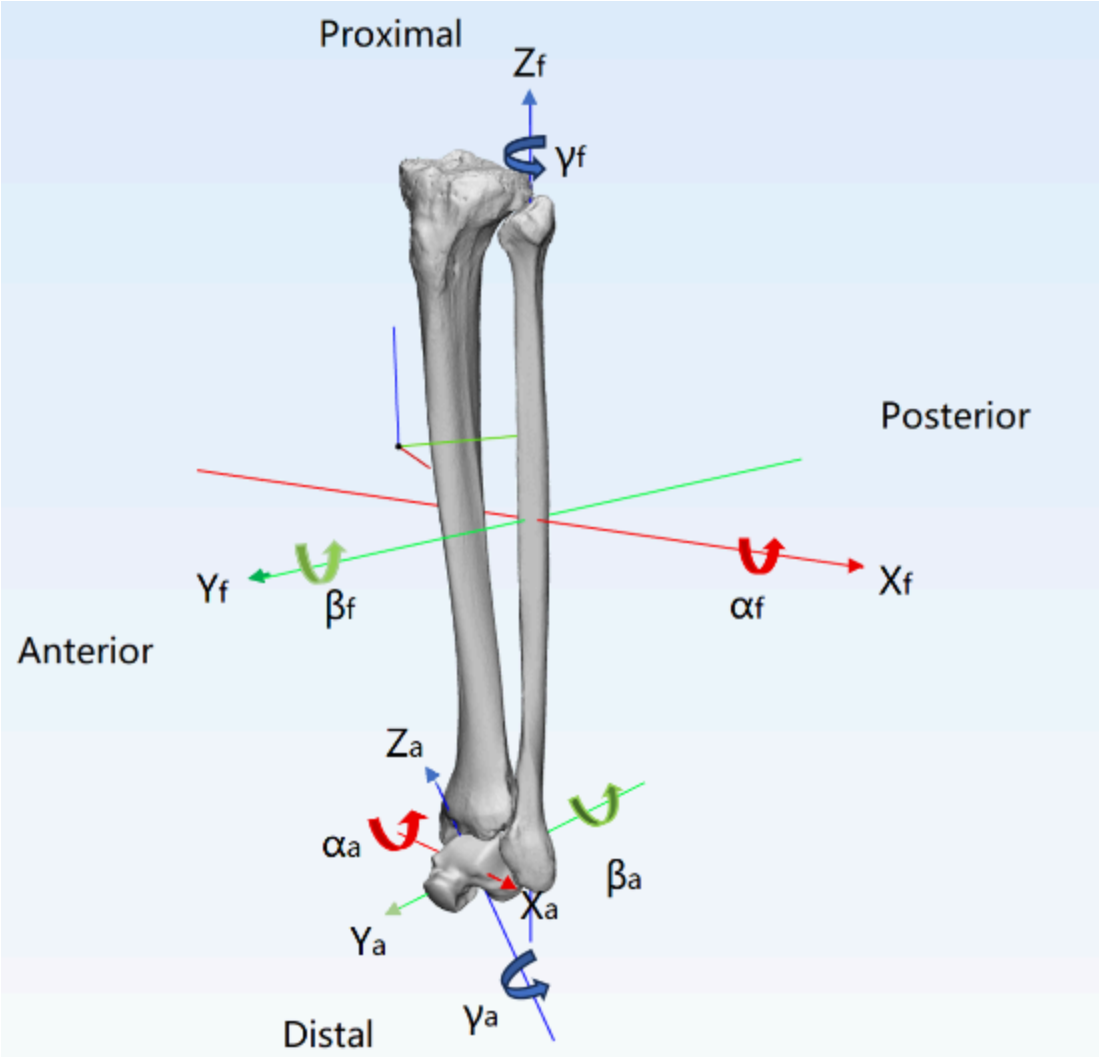


Figure 5

f: Fibula, a: Talus. X-axis: External rotation (+)/Internal rotation (-), Y-axis: Anterior movement (+)/Posterior movement (-), Z-axis: Upward movement (+)/Downward movement (-), α: Plantar flexion (-)/Dorsiflexion (+), β: Inversion (-)/Eversion (+), γ: External rotation (-)/Internal rotation (+).

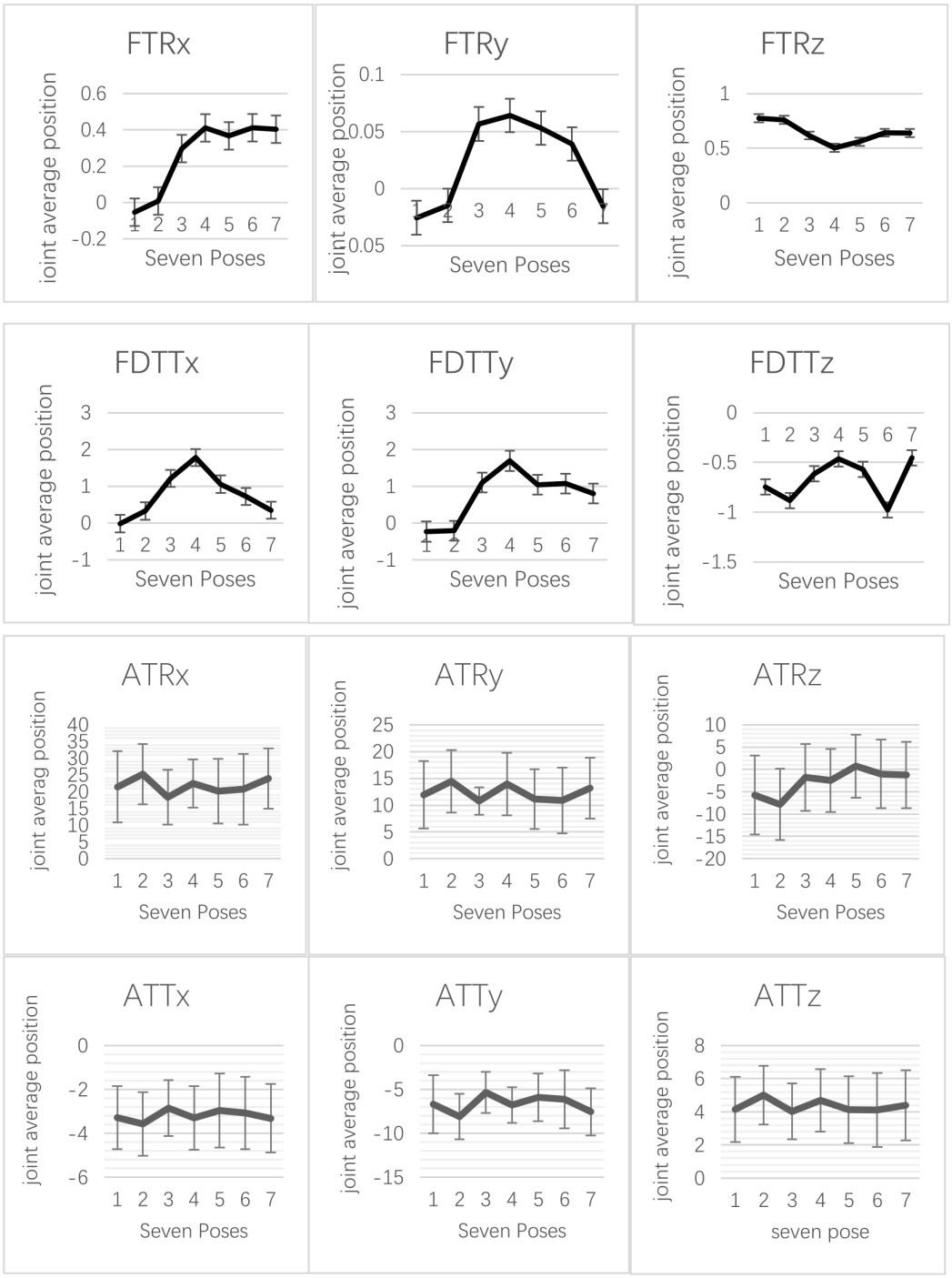


Figure 6. Average position movement pattern of the fibula and the talus during the gait cycle: F:fibula;A:talus;TRx: dorsiflexion (+)/plantarflexion (-); TRy: eversion (+)/inversion (-); TRz: internal rotation (+)/external rotation (-); TTx: lateral (+)/medial (-) translation; TTy: anterior (+)/posterior (-) translation; TTz: superior (+)/inferior (-) translation.

Figure 6

See image above for figure legend